Cytotoxic and Apoptotic Effects of Olive Leaf Extract Chitosan Nanoparticles on Breast Cancer MCF-7 and Lung Cancer A549 Cells

Burcu Özdamar
Izmir Institute of Technology: Izmir Yuksek Teknoloji Enstitusu
Yusuf Sürmeli
Izmir Institute of Technology: Izmir Yuksek Teknoloji Enstitusu
Gülşah Şanlı Mohamed (gulsahsanli@iyte.edu.tr)
Izmir Institute of Technology: Izmir Yuksek Teknoloji Enstitusu

Research Article

Keywords: Olive leaf extract (OLE), chitosan nanoparticles, MCF-7, A549, apoptosis, cytotoxic effects

Posted Date: November 4th, 2022

DOI: https://doi.org/10.21203/rs.3.rs-2209453/v1

Abstract

I. Background

Chitosan, which is a biocompatible and nontoxic material, is predominantly used as a polymer having the ability to nanoparticle formation. In this work, we immobilized olive leaf extract (OLE) with chitosan nanoparticles (CNPs), and elaborately characterized the OLE-CNPs. Also, the cytotoxic influence, the cell cycle distribution, and apoptosis stage of OLE and OLE-CNPs were analyzed on lung carcinoma (A549) and breast adenocarcinoma (MCF-7).

II. Methods and Results

OLE-CNPs were characterized by Zetasizer Nano-ZS and FT-IR Spectrometer. The cytotoxic effects of OLE-CNPs were performed by MTT assay, and cell cycle distribution and apoptotic effects of OLE-CNPs were carried out by using flow cytometer. The loading capacity and the size of OLE-loaded nanoparticles were found as 97.5% and about 100 nm, respectively, in the optimum conditions. In addition, OLE-CNPs were characterized by unique FTIR peaks and morphological display compared to the CNPs. *In vitro* cytotoxic assay indicated that IC_{50} values of OLE-CNPs were determined as 540 μg/mL for A549 and 810 μg/mL for MCF-7. The treatment of both A549 and MCF-7 with OLE-CNPs caused the highest cell arrest in G0/G1 in a dose-independent manner. OLE-CNPs affected cell cycle distribution different from free OLE treatment in both cancer cells. A549 and MCF-7 cells were predominantly found in the late apoptosis and necrosis phase, respectively, upon treatment of 1000 μM OLE-CNPs.

III. Conclusions

Our results suggest that CNPs enhance bioavailability OLE as nutraceuticals in cancer and OLE-CNPs might be offered as supplements for cancer therapy.

1. Introduction

Nanotechnology has a wide variety of applications in the medical, industrial, and genetic sciences, and with the use of nanotechnology, the scope of many researches has radically changed [1–3]. Nanomaterials used in nanotechnology can be in a broad diversity of physical and chemical properties such as diameters, shapes, and surface structure [4]. They are utilized in different applications including anticancer drugs, antimicrobials, and drug delivery [5–7].

Among nanomaterials, chitosan is a biocompatible and nontoxic material and is largely utilized as a polymer having the ability to nanoparticle formation [8]. Chitosan is a biopolymer obtained from chitin, which is a structural component of crustacean shells, the cell wall of fungi, and insect cuticles [9], and it is composed of a linear polysaccharide structure of D-glucosamine and N-acetyl-D-glucosamine residues with the linkage of β-(1–4) glycosidic bonds [10]. Also, it possesses some beneficial properties (e.g.

highly stable, biologically degradable, and sufficient permeable), which enable chitosan to use as an ideal biological polymer in medical applications [11, 12].

Olea europaea, the olive tree, has had an important place in the herbal medicine of Mediterranean and European countries for many years [13]. Olive leaf possesses a range of therapeutic features including anticancer, antioxidant, antimicrobial, antiviral (e.g. SARS CoV-2), anti-inflammatory, as well as cardioprotective, neuroprotective, and hepatoprotective [14–16]. Olive leaf extract (OLE) is rich in phenolics such as oleuropein, apigenin, and hydroxytyrosol [14]. The rapid oxidation occurs in phenolics, thus leading to tarnishing, unpleasant taste and odor, and a considerable decrease in efficacy. Therefore, it is suggested that they should be covered with the material before their use as oral drugs or supplements in foodstuffs [17].

There have been few studies on the immobilization of tree leaf extracts used in herbal medicine with chitosan and their effects on cancer cells. The immobilization of leaf extract of Annona squamosa, a custard apple, with chitosan nanoparticles (nano-ASLE) had a cytotoxic effect, and induced apoptosis in human colon cancer (WiDr) and HeLa cells [18, 19]. Also, another recent work has shown that the immobilization of leaf extract of Dendrophthoe pentandra, a mango-growing parasitic plant, with chitosan had a cytotoxic effect on the G2/M cell cycle arrest in MCF-7 breast cancer cells [20]. To the best of our knowledge, no research has been reported on OLE-loaded chitosan nanoparticles (OLE-CNPs) thus far. In the present work, we immobilized the OLE with chitosan nanoparticles and characterized OLE-CNPs by the Folin-Ciocalteu method, FTIR, AFM, and Zeta Sizer Nano-ZS. Then, we investigated the influence of OLE-CNPs on lung carcinoma (A549) and breast adenocarcinoma (MCF-7) cell lines.

2. Materials And Methods

2.1. Materials

Olive leaves were supplied from Olive Research Institute (İzmir, Turkey). Unless otherwise stated all chemicals including chitosan (CS) and sodium tripolyphosphate (TPP) were purchased from Sigma.

2.2. Extraction of olive leaves

Olive leaves extraction was carried out according to the procedure below: olive leaves were cleaned using dH_2O, incubated at 37°C-72 h for drying and powdered, and extracted 70% ethanol at 25^{o}C-2 h. The liquid phase including ethanol was removed using a vacuum filter and a rotary evaporator at 38°C-120 rpm, respectively. Olive leaves extract (OLE) was dried using a freeze-dryer in the presence of -52°C-0.2 mbar conditions. It was stored in a light-protected bottle.

2.3. OLE characterization

2.3.1. Determination of total phenolic content

The total phenolic content of OLE was investigated through the Folin-Ciocalteu procedure as explained by Bayçın et al. [21]. In brief, OLE was dissolved in dH_2O, and 20 µl of the sample was added to the 100 µl of Folin reagent using a 96-well plate upon incubation of 2 min at room temperature (RT). Then, 80 µl of 7% Na_2CO_3 was supplemented into the mixture and the mixture was incubated for 60 min. The spectrophotometric measurement of the samples was performed at OD_{725}. This analysis was carried out in triplicate and the results were expressed as milligrams of gallic acid equivalents per gram of dry olive leaf (mg GAE/g) using a gallic acid calibration curve.

2.3.2. OLE composition investigation

OLE composition was investigated by HPLC analysis using Hewlett-Packard Series HP 1100 equipped with a diode array detector and C18 LiChrospher 100 analytical column (250 mm×4 mm). The flow rate was 1 ml/min and the absorbance change was monitored at OD_{280}. 2.5/97.5 (v/v) of acetic acid/water (A) and acetonitrile (B) were utilized as mobile phases and a linear gradient was applied for 60 min, as 20 min from 95% A-5% B to 75% A-25% B, 20 min at 50% A-50% B and 10 min at 20% A-80% B, respectively. Finally, re-equilibration of the system was carried out for 10 min and the system had the initial composition.

Oleuropein extent of OLE was also investigated via HPLC assay utilizing an oleuropein calibration curve. coumarin as an internal standard was used to measure the antioxidant oleuropein.

2.3.3. Antioxidant capacity test

Trolox Equivalent Antioxidant Capacity (TEAC) test was carried out to investigate the total antioxidant capacity of the OLE. To do this, sodium persulfate ($K_2S_2O_4$) was added to 2,2'-azinobis-(3-ethylbenzothiazoline-6-sulfonic acid) (ABTS+) working solution at an equal amount and then incubated at RT in dark along 12 to16 h. The mixture was spectrophotometrically measured at 734 nm wavelength. The results were expressed as mmol TEAC/g OLE of the sample using a Trolox calibration curve.

2.4. Preparation and optimization of OLE-CNPs

The chitosan nanoparticles were synthesized by the following procedure; 0.5% chitosan dissolved in 1% (w/v) acetic acid solution was incubated at 115 rpm until it was transparent and adjusted to pH 5.0. 0.25% OLE was supplemented into chitosan solution and the mixture was incubated for 30 min. Then, the sodium tripolyphosphate (TPP) solution (0.1%) was added to the mixture and was stirred at RT for 1 h. The mixture was centrifuged at 13500 rpm for 30 min and Freeze-dried nanoparticles were stored at 4^oC for further analyses. The loading capacity of OLE-CNPs was optimized by investigation of the effect of various conditions including TPP concentrations (0.08-3%), pH (4–5), incubation time of TPP (15–120 min), and the OLE (15–120 min), and OLE concentration (0.1-2%).

The loading capacity of the nanoparticles was calculated using the equation below:

$$\%LC=(A-B)/A\times100$$

Where "A" is the total amount of OLE; "B" is the free amount of OLE.

2.5. Characterization of the OLE-CNPs

The loading capacity of the nanoparticles was investigated using the Folin-Ciocalteu method by spectrophotometric analysis [22]. In addition, the morphology of the nanoparticles was characterized by Nanomagnetic Instruments ezAFM on Tapping mode. The nanoparticle size was carried out by using a Zetasizer Nano-ZS (Malvern Instruments) based on dynamic light scattering (DLS) techniques. The interactions between the chitosan nanoparticles and the OLE were analyzed by Fourier transform infrared spectroscopy (FT-IR) according to the Miracle Zn-Se ATR method on a Spectrum-100 FT-IR Spectrometer (Perkin Elmer) in the range of 650–4000 cm^{-1}

2.7. The influence of OLE-CNPs on cancer cell lines

2.7.2. The cytotoxicity analysis

The cytotoxicity analysis was carried out for testing the various concentrations of OLE-CNPs against MCF-7 (breast adenocarcinoma), BEAS 2B (human bronchial epithelium), and A549 (lung carcinoma) by MTT assay. To do this, 1 x 10^4 cells/mL of each cell line was cultured using 96-well plates and incubated for 24 h. The cells were subjected to a concentration range of 1-1000 µg/mL of OLE and OLE-CNPs. The incubation of the treated and the control cells was performed at 37°C for 72 h. Then, the cultures were washed with PBS buffer, 100 µL of 10% MTT was added to each well, and plates were incubated at 37°C, 5% CO_2 for 4 h. The cultures were centrifuged at 1800 rpm for 10 min and the pellets were dissolved in DMSO. The absorbance of the samples was spectrophotometrically measured at 540 nm wavelength. The percent cell viability was expressed as the ratio of the absorbance of the treated cells to the untreated (control) cells multiplied by 100. The concentration inhibiting cell viability by 50% (IC_{50}) was calculated by a standard curve of cell viability. This assay was carried out in triplicate.

2.7.3. Cell cycle assay

Anti-proliferative action of free OLE and OLE-CNPs on the cell cycle of MCF-7 and A549 was investigated using flow cytometry with propidium iodide (PI) staining as fluorescent staining. For this purpose, A549 and MCF-7 cells were cultured into 6-well plates including a 1.98 mL growth medium at a density of 1x10^5 cells/well and grown overnight. Then, 20 µL of free OLE and OLE-CNPs were added into each well in a concentration range of 300 – 100 µg/mL for A-549 and 100–1000 µg/mL for MCF-7 cell lines. The cultures were incubated at 37°C and 5% CO_2 condition for 72 h. The cells were fixed using trypsin, PBS, and cold ethanol, respectively. The fixed cells were harvested at 4°C-1200 x g for 10 min by centrifugation. The cell pellets were treated with the 200 µL of Triton X-100 (0.1%) and 20 µL of RNase A (200 µg/mL), respectively, and the cell suspensions were then incubated at 37°C-5% CO_2 condition for 30 min. After the addition of 20 µL of 1 mg/mL PI, the samples were incubated at room temperature for 15 min. The cell cycle distribution was determined by a flow cytometer (FACSCANTO, BD). The obtained data was analyzed by ModFit software and was collected for a minimum of 10.000 events for each sample.

2.7.4. The apoptotic effect of OLE-CNPs on cancer cells

The apoptotic effect of OLE-CNPs on MCF-7 and A549 was investigated using Annexin V- FITC Detection Kit. Briefly, the cancer cells were cultured onto a 6-well plate with a 1.98 mL growth medium at a density of 1 x 10^5 cells/well and incubated at 37°C and 5% CO_2 for 24 h. The cell cultures were then subjected to 20 µL of the OLE-CNPs in a concentration range of 100 to 1000 µg/mL. The treated and the control cell cultures were incubated at 37°C and 5% CO_2 for 48 h. The cultures were two times harvested at 800 rpm for 5 min, washed with PBS, and the pellets were resuspended in 200 µL binding buffer. 2 µL of annexin V-FITC and PI were then supplemented, and the stained cells were incubated at room temperature for 15 min and the mixtures were analyzed using flow cytometer (FACSCANTO, BD).

2.7.5. Optical microscopy display

The influence of the free OLE and the OLE-CNPs was monitored using optical microscopy. For this purpose, MCF-7 and A549 cell cultures were prepared with a 96-well plate and incubated overnight. The cytotoxic concentration of free OLE and OLE-CNPs was supplemented into each well including the MCF-7 or A549 cell culture and the plate was incubated for 72 h. Finally, the cells were monitored by optical microscopy.

3. Results And Discussion

In this work, OLE was immobilized by chitosan nanoparticles, and OLE-CNPs were optimized, characterized, and investigated the influence on cancer cells (breast adenocarcinoma MCF-7, and lung carcinoma A549) and healthy cells (human bronchial epithelium cells BEAS 2B). To do this, OLE was characterized to detect the total antioxidant capacity and the total phenolic content. Antioxidant capacity was found as 2.18 mmol of TEAC/g OLE and the total phenolic content of OLE was calculated as 260 mg GAE/g extract. Recent work has shown that the TPC value of Chinese olive (*Olea europaea*) leaves was found as 197.32 mg/g of dry matter [23]. Another study has shown that the leaves of ten major Greek olive varieties possessed total phenolic content of up to 20 mg GAE/g tissue [24].

3.1. Optimization of OLE-CNPs

OLE was immobilized by using chitosan nanoparticles and the loading capacity of OLE-CNPs was optimized by investigation of the effect of various conditions including chitosan-TPP mass ratio (1:1, 1:2, 1:3, 1:4, 1:5, 1:6, 2:1, 3:1, 4:1, 5:1 and 6:1), pH (4, 4.3, 4.6, 4.7, and 5.0), incubation time of TPP (15, 30, 60, 90, and 120 min) and the OLE (15, 30, 60, 90, and 120 min), and OLE concentration (0.1%, 0.25%, 0.5%, 1.0%, and 1.5%). The size distribution of OLE-CNPs was also determined by Zetasizer Nano-ZS (Malvern Instruments) based on dynamic light scattering (DLS) techniques in the above-mentioned conditions. The analyses showed that the optimal conditions were determined as 5:1 chitosan-TPP mass ratio, pH 5.0 of Tris-HCl buffer, 60 min incubation time of TPP, 30 min of OLE incubation time, and 0.25% of OLE concentration (Fig. 1).

3.2. Characterization of OLE-CNPs

OLE-CNPs were characterized in terms of loading capacity, size, morphology, and interactions between OLE and chitosan nanoparticles. The loading capacity and the size of OLE-loaded nanoparticles were found as 97.5% and about 100 nm, respectively, in the optimum conditions. In addition, the morphology of OLE-CNPs was analyzed by Nanomagnetic Instruments ezAFM on Tapping mode. OLE-CNPs were more spherical, compared to the chitosan nanoparticles, lacking the pronounced morphological differences (Figs. 2a and 2b). Also, the interactions between OLE and chitosan nanoparticles in OLE-CNPs were analyzed using FTIR spectroscopy, relative to the chitosan nanoparticles. When the OLE-CNPs spectra were compared with spectra of CNPs, shifted bands were observed from 3449 cm^{-1} to 3336.7 cm^{-1} as a result of H-bonding that occurs between the OLE and CS matrix. Stretching vibration of $-NH_2$ and –OH groups were shifted to 3154.4 cm^{-1}. In addition to this situation, the characteristic $-NH_2$ band disappeared. The disappearance of the band could be attributed to the linkage between the –OH groups of TPP and ammonium ions of chitosan (Fig. 2c).

3.3. The effect of OLE-CNPs on cancer cell lines

3.3.1. In vitro cytotoxicity analysis

Cytotoxicity of various concentrations of OLE-CNPs, CNPs, chitosan, and OLE on two cancer cell lines (A549 and MCF-7), and a healthy cell line (BEAS 2B) was investigated by MTT assay. The analysis indicated that the cell viability of three cell lines was over 80% against 1000 µg/mL of free OLE (Fig. 3). Similarly, the cell viability of three cell lines was over 75% against 1000 µg/mL of chitosan. It was shown that chitosan nanoparticles had more toxic effects on all cell lines, exhibiting viability in a range of 42%-61%. In addition, 1000 µg/mL of OLE-CNPs considerably reduced the viability of the cell lines to 20% of A549 (Fig. 3a), 16% of MCF-7 (Fig. 3b), and 5.5% of BEAS-2B (Fig. 3c). IC_{50} of OLE-CNPs was found as 540 µg/mL for A549 and 810 µg/mL for MCF-7. To the best of our knowledge, there have been no works on the effect of OLE-immobilized chitosan nanoparticles against A549 and MCF-7. However, there have been studies on the immobilization of leaf extracts of different medicinal plants with chitosan and their effects on cancer cells. Regarding this, the immobilization of leaf extract of *Dendrophthoe pentandra*, a mango-growing parasitic plant with chitosan (NPDP), has a high cytotoxic effect on MCF-7 cells, exhibiting about 20% of cell viability at 8 mg/mL concentration [20]. Another recent study has shown that *Annona squamosa* (named Srikaya belonging to Annonaceae family) leaf extract-loaded chitosan (nano-ASLE) has an IC_{50} of 344.48 µg/mL on HeLa cells [19]. There has been a recent study on the effects of OLE immobilization with different support materials on the MCF-7 cell line. For instance, OLE-loaded silver nanoparticles (AgNPs) decreased the cell viability of MCF-7 by 62% at 50 µg/mL [25].

3.3.2. The cell cycle distribution of cancer cell lines against OLE and OLE-CNPs

Cell cycle distribution of A549 and MCF-7 treated by various concentrations (10, 100, 500, 1000 μM) of free OLE and OLE-CNPs was analyzed by flow cytometer. The analysis indicated that an increase of OLE-CNP concentrations, but not free OLE, gradually diminished the A549 cell number in G2/M arrest from 16–5.5%. Similarly, the A549 cell number decreased in G0/G1 from 77–40% and raised in the S phase from 12–55%, to a gradual increase of OLE-CNPs concentration. Free OLE did not considerably change the cell cycle distribution and exhibited a concentration-independent manner in A549 cells. The analysis also showed that OLE-CNPs behaved in a dose-dependent manner in all phases (Fig. 4A). MCF-7 treated with OLE-CNPs showed higher cell percent in the G2/M phase and lower in the S phase, relative to the free OLE. Free OLE and OLE-CNP treatment exhibited a similar cell percent in the G0/G1 phase of MCF-7 (Fig. 4B). In literature, *Dendrophthoe pentandra* leaf extract-loaded chitosan (NPDP) nanoparticles induced the G2/M cell cycle arrest in MCF-7 cancer cells [20]. Similarly, *Annona squamosa* leaf extract-loaded chitosan (nano-ASLE) also stimulated the cell cycle arrest in G2/M in WiDr cancer cells [18]. The present study showed that both cancer cells were predominantly distributed in the G0/G1 phase in the presence of OLE-CNP and free OLE (Fig. 4). These results were supported by some works on free OLE-treated or some OLE ingredients (e.g. hydroxytyrosol and oleuropein)-treated MCF-7 cancer cells showing the cell cycle distribution in G0/G1 arrest [26].

3.3.3. Apoptotic influence of OLE-CNPs on cancer cell lines

The apoptotic influence on A549 and MCF-7 cancer cells treated with different concentrations of OLE-CNPs (50, 100, 300, 500, and 1000 μM), relative to nontreated cells, were analyzed using the Annexin V/propidium iodide (PI) staining method. The analysis showed that the viable A549 cell percent treated with OLE-CNPs decreased, compared to the nontreated cells. In contrast, the cell percent in necrosis and late apoptosis phase is enhanced with an increase in OLE-CNPs concentration (Fig. 5A). MCF-7 viable cell percent decreased by about 40% at 1000 μM concentration of OLE-CNPs, relative to the non-treated cells. Also, cell percent in the necrosis phase did not significantly change up to 500 μM concentration; however, at 1000 μM concentration, the cell percent increased by 55–70% (Fig. 5B). These results suggest that OLE-CNPs strongly induced apoptosis and necrosis in A549 and MCF-7 cells. Anbu et al. (2016) have shown that the leaf extract of the medicinal plant *Gymnema sylvestre* with chitosan nanoparticles led to apoptosis in human cervical cancer (SiHa) cell line [27]. In addition, nano chitosan encapsulation of *C. citratus* leaf ethanol extract (NCECC) promoted ROS production, causing apoptosis in human squamous cells (HSC-3) [28]. Another recent study has shown that nano-ASLE significantly enhanced the caspase-3 expression and caused apoptosis in WiDr cells [18].

According to the optical microscopy analyses, the reduction in A549 and MCF-7 cell numbers was displayed in the presence of OLE-CNPs, relative to the other conditions. Shrinking the cell and forming the apoptotic bodies were seen in the OLE-CNP-treated cells. This result was consistent with the cytotoxicity results of the OLE-CNPs on both cells (Figs. 5C and 5D).

4. Conclusion

In this study, olive leaves of *Olea europaea* were extracted, immobilized, characterized, and investigated the influences on breast adenocarcinoma MCF-7 and lung carcinoma A549. The present work was the first report on the immobilization of olive leaf extract (OLE) with chitosan nanoparticles (CNP). The results showed that the loading capacity and size of OLE-CNPs were determined as about 97.5% and 100 nm, respectively, under optimal conditions. Also, cytotoxicity results indicated that OLE-CNPs had higher cytotoxic influences on A549 and MCF-7 cell lines, compared to the free OLE. IC_{50} of OLE-CNPs on A549 and MCF-7 was found as 540 µg/mL and 810 µg/mL, respectively. The cell cycle distribution assay showed that above half of the A549 and MCF-7 cells exposed to free OLE and OLE-CNP accumulated in the G0/G1 phase. Apoptosis results demonstrated that OLE-CNPs caused the accumulation of the A549 and MCF-7 cells in the late apoptosis and necrosis phases. Based on the present work results, OLE-CNPs might be offered as supplements for cancer therapy.

Declarations

Acknowledgment

The authors would like to thank Biotechnology & Bioengineering Research Center at İzmir Institute of Technology for the facilities and technical support.

Conflict of interest

The authors declare no competing interests.

Ethical approval

This article does not contain any studies with human participants or animals performed by any of the authors.

References

1. Albrecht MA, Evans CW, Raston CL (2006) Green chemistry and the health implications of nanoparticles. Green Chem 8(5):417–432. https://doi.org/10.1039/B517131H
2. Zheng J, Stevenson MS, Hikida RS, Van Patten PG (2002) Influence of pH on dendrimer-protected nanoparticles. J Phys Chem B 106(6):1252–1255. https://doi.org/10.1021/JP013108P/SUPPL_FILE/JP013108P_S.PDF
3. Khan SA, Noreen F, Kanwal S, Iqbal A, Hussain G (2018) Green synthesis of ZnO and Cu-doped ZnO nanoparticles from leaf extracts of Abutilon indicum, Clerodendrum infortunatum, Clerodendrum inerme and investigation of their biological and photocatalytic activities. Mater Sci Engineering: C 82:46–59. https://doi.org/10.1016/J.MSEC.2017.08.071
4. Raveendran P, Fu J, Wallen SL (2003) Completely “green” synthesis and stabilization of metal nanoparticles. J Am Chem Soc 125(46):13940–13941.

https://doi.org/10.1021/JA029267J/SUPPL_FILE/JA029267JSI20030324_031335.PDF

5. Rajeshkumar S (2016) Anticancer activity of eco-friendly gold nanoparticles against lung and liver cancer cells. J Genet Eng Biotechnol 14(1):195–202. https://doi.org/10.1016/J.JGEB.2016.05.007
6. Dorosti N, Jamshidi F (2016) Plant-mediated gold nanoparticles by Dracocephalum kotschyi as anticholinesterase agent: Synthesis, characterization, and evaluation of anticancer and antibacterial activity. J Appl Biomed 14(3):235–245. https://doi.org/10.1016/J.JAB.2016.03.001
7. Ghorbani M, Hamishehkar H (2017) Redox and pH-responsive gold nanoparticles as a new platform for simultaneous triple anti-cancer drugs targeting. Int J Pharm 520(1–2):126–138. https://doi.org/10.1016/J.IJPHARM.2017.02.008
8. Ding RL, Xie F, Hu Y, Fu SZ, Wu JB, Fan J, He WF, He Y, Yang LL, Lin S, Wen QL (2017) Preparation of endostatin-loaded chitosan nanoparticles and evaluation of the antitumor effect of such nanoparticles on the Lewis lung cancer model. Drug Deliv 24(1):300–308. https://doi.org/10.1080/10717544.2016.1247927
9. Crini G (2006) Non-conventional low-cost adsorbents for dye removal: A review. Bioresour Technol 97(9):1061–1085. https://doi.org/10.1016/J.BIORTECH.2005.05.001
10. Zhao QS, Ji QX, Xing K, Li XY, Liu CS, Chen XG (2009) Preparation and characteristics of novel porous hydrogel films based on chitosan and glycerophosphate. Carbohydr Polym 76(3):410–416. https://doi.org/10.1016/J.CARBPOL.2008.11.020
11. Sarkar S, Guibal E, Quignard F, SenGupta AK (2012) Polymer-supported metals and metal oxide nanoparticles: synthesis, characterization, and applications. J Nanoparticle Res 14(2):1–24. https://doi.org/10.1007/S11051-011-0715-2
12. Abdelsalam NR, Abdel-Megeed A, Ali HM, Salem MZM, Al-Hayal MFA, Elshikh MS (2018) Genotoxicity effects of silver nanoparticles on wheat (Triticum aestivum L.) root tip cells. Ecotoxicol Environ Saf 155:76–85. https://doi.org/10.1016/J.ECOENV.2018.02.069
13. El SN, Karakaya S (2009) Olive tree (Olea europaea) leaves: potential beneficial effects on human health. Nutr Rev 67(11):632–638. https://doi.org/10.1111/J.1753-4887.2009.00248.X
14. Morandi F, Bensa V, Calarco E, Pastorino F, Perri P, Corrias MV, Ponzoni M, Brignole C (2021) The olive leaves extract has anti-tumor effects against neuroblastoma through inhibition of cell proliferation and induction of apoptosis. Nutrients 13(7):2178. https://doi.org/10.3390/NU13072178
15. Ünlü AE (2021) Green and non-conventional extraction of bioactive compounds from olive leaves: screening of novel natural deep eutectic solvents and investigation of process Parameters. Waste Biomass Valorization 12(10):5329–5346. https://doi.org/10.1007/S12649-021-01411-3/TABLES/8
16. Kermanshah Z, Samadanifard H, Moradi Moghaddam O, Hejrati A (2020) Olive leaf and its various health-benefitting effects: a review study. Pakistan J Medical Health Sci 14(2):1301–1312
17. Munin A, Edwards-Lévy F (2011) Encapsulation of natural polyphenolic compounds; a review. Pharmaceutics 3(4):793. https://doi.org/10.3390/PHARMACEUTICS3040793
18. Fadholly A, Proboningrat A, Dewi Iskandar R, Rantam F, Sudjarwo S (2019) In vitro anticancer activity Annona squamosa extract nanoparticle on WiDr cells. J Adv Pharm Technol Res 10(4):149.

https://doi.org/10.4103/JAPTR.JAPTR_10_19

19. Fadholly A, Ansori ANM, Proboningrat A, Nugraha AP, Iskandar RPD, Rantam FA, Sudjarwo SA (2020) Apoptosis of HeLa cells via caspase-3 expression induced by chitosan-based nanoparticles of Annona squamosa leaf extract: In vitro study. Indian J Pharm Educ Res 54(2):416–421. https://doi.org/10.5530/ijper.54.2.47
20. Permana S, Lukman H, Norahmawati E, Eka Puspita O, Faisal Moh Al Zein D, Kawamoto Y, Tri Endharti A (2021) The combination therapy of targeting both paclitaxel and Dendrophthoe pentandra leaves extract nanoparticles for improvement breast cancer treatment efficacy by reducing TUBB3 and MAP4 expressions. Acta Biochim Pol. https://doi.org/10.18388/ABP.2020_5563
21. Bayçin D, Altiok E, Ülkü S, Bayraktar O (2007) Adsorption of olive leaf (Olea europaea L.) antioxidants on silk fibroin. J Agric Food Chem 55(4):1227–1236. https://doi.org/10.1021/JF062829O
22. Singleton VL, Orthofer R, Lamuela-Raventós RM (1999) Analysis of total phenols and other oxidation substrates and antioxidants by means of folin-ciocalteu reagent. Methods Enzymol 299:152–178. https://doi.org/10.1016/S0076-6879(99)99017-1
23. Wang B, Shen S, Qu J, Xu Z, Feng S, Chen T, Ding C (2021) Optimizing total phenolic and oleuropein of Chinese olive (Olea europaea) leaves for enhancement of the phenols content and antioxidant activity. Agronomy 11(4):686. https://doi.org/10.3390/AGRONOMY11040686
24. Mitsopoulos G, Papageorgiou V, Komaitis M, Hagidimitriou M (2016) Total phenolic content and antioxidant activity in leaves and drupes of ten olive varieties. Not Bot Horti Agrobot 44(1):155–161. https://doi.org/10.15835/NBHA44110381
25. De Matteis V, Rizzello L, Ingrosso C, Liatsi-Douvitsa E, De Giorgi ML, De Matteis G, Rinaldi R (2019) Cultivar-dependent anticancer and antibacterial properties of silver nanoparticles synthesized using leaves of different Olea europaea trees. Nanomaterials 9(11). https://doi.org/10.3390/NANO9111544
26. Bouallagui Z, Han J, Isoda H, Sayadi S (2011) Hydroxytyrosol rich extract from olive leaves modulates cell cycle progression in MCF-7 human breast cancer cells. Food Chem Toxicol 49(1):179–184. https://doi.org/10.1016/J.FCT.2010.10.014
27. Sujima Anbu A, Velmurugan P, Lee JH, Oh BT, Venkatachalam P (2016) Biomolecule-loaded chitosan nanoparticles induce apoptosis and molecular changes in cancer cell line (SiHa). Int J Biol Macromol 88:18–26. https://doi.org/10.1016/J.IJBIOMAC.2016.03.042
28. Andikoputri SF, Komariah K, Roeslan MO, Ranggaini D, Bustami DA (2021) Nano chitosan encapsulation of Cymbopogon citratus leaf extract promotes ROS induction leading to apoptosis in human squamous cells (HSC-3). Curr Issues Pharm Medical Sci 34(3):134–137. https://doi.org/10.2478/CIPMS-2021-0026

Figures

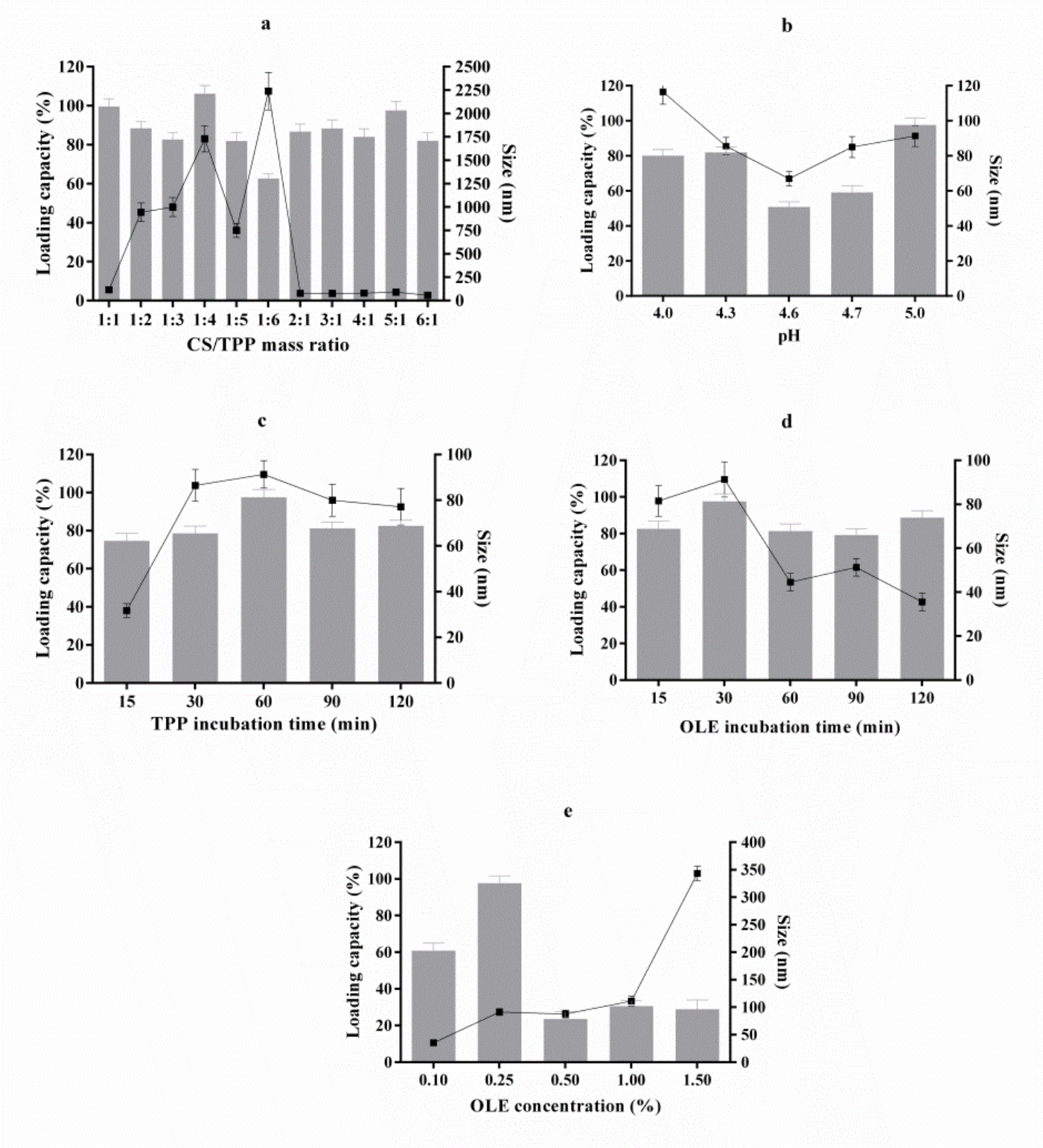

Figure 1

The optimization of loading capacity and chitosan nanoparticle sizes in various conditions including (a) chitosan-TPP mass ratio, b) pH of Tris-HCl buffer, c) incubation time of TPP, d) incubation time of OLE, e) OLE concentration. (Lines refer to nanoparticle size, and columns refer to loading capacity).

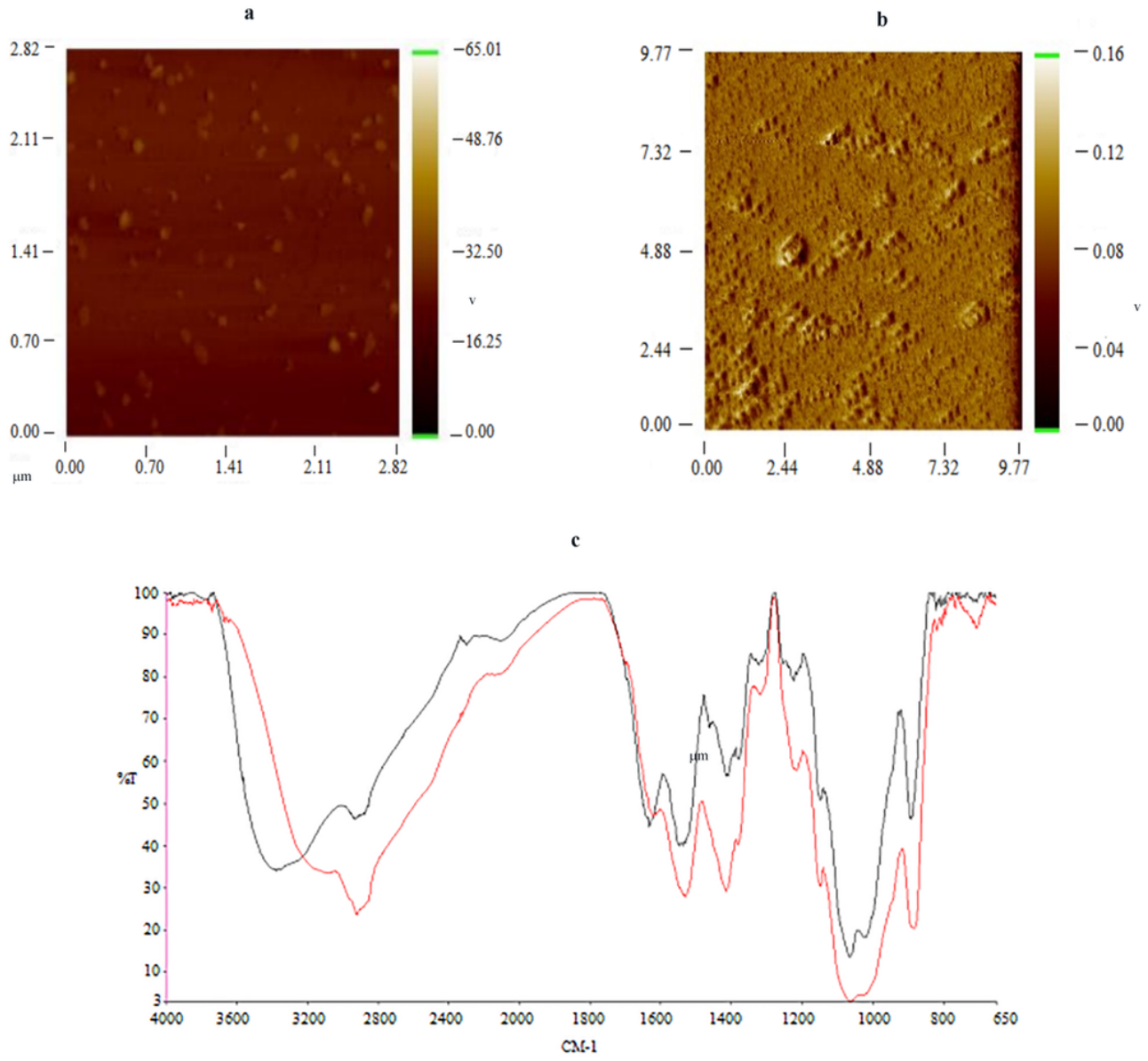

Figure 2

Characterization of the OLE-CNPs a) AFM image of chitosan nanoparticles, b) AFM image of OLE-CNPs c) FTIR spectra of OLE-CNPs and CNPs. The red line belongs to OLE-CNP, and the black line belongs to CNP)

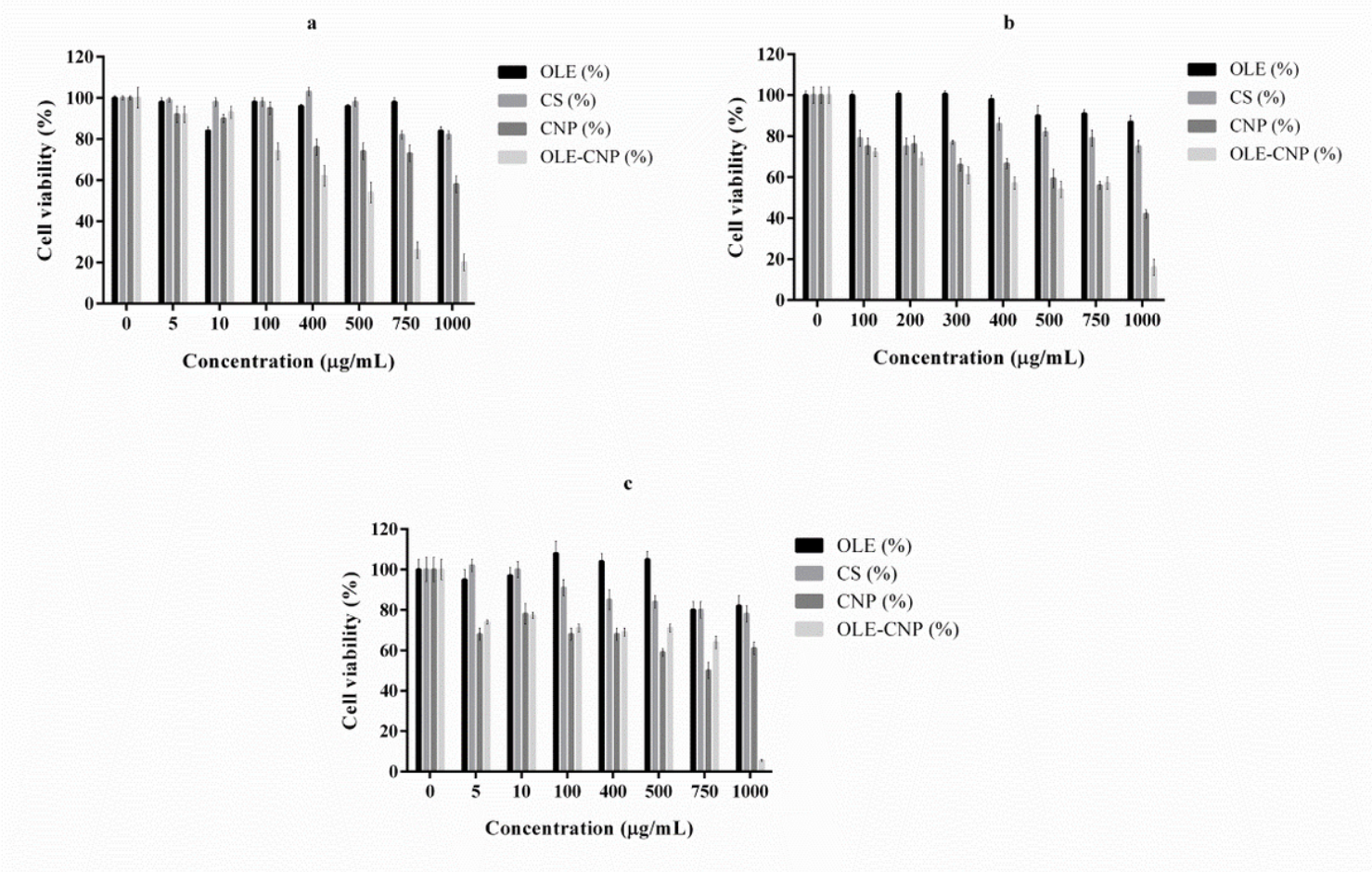

Figure 3

The cytotoxicity of OLE, chitosan (CS), chitosan nanoparticles (CNPs), and OLE-CNPs against (a) A549, (b) MCF-7, and (c) BEAS 2B.

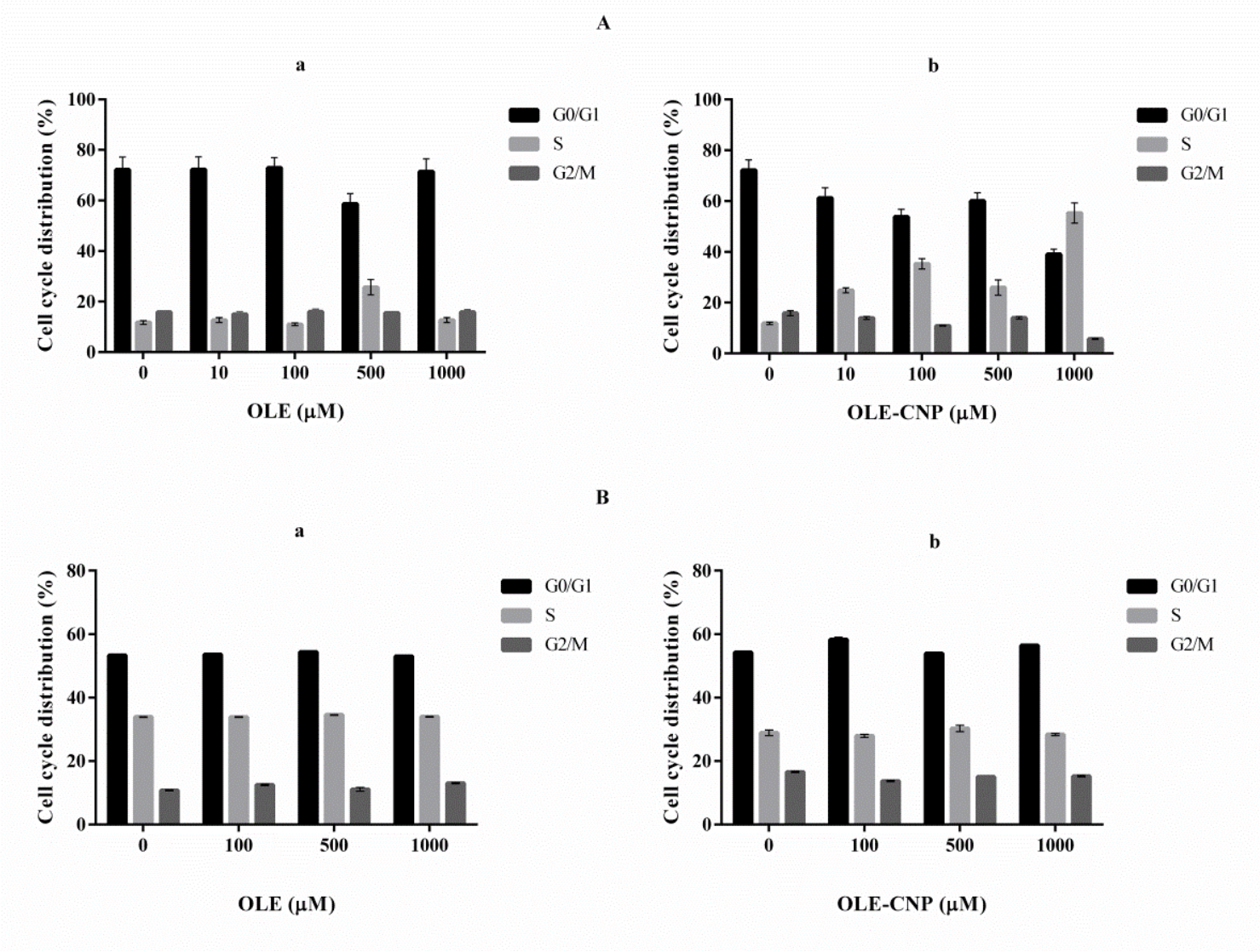

Figure 4

The effect of OLE (a) and OLE-CNPs (b) on cell cycle arrest in A549 (A) and MCF-7 (B) cells.

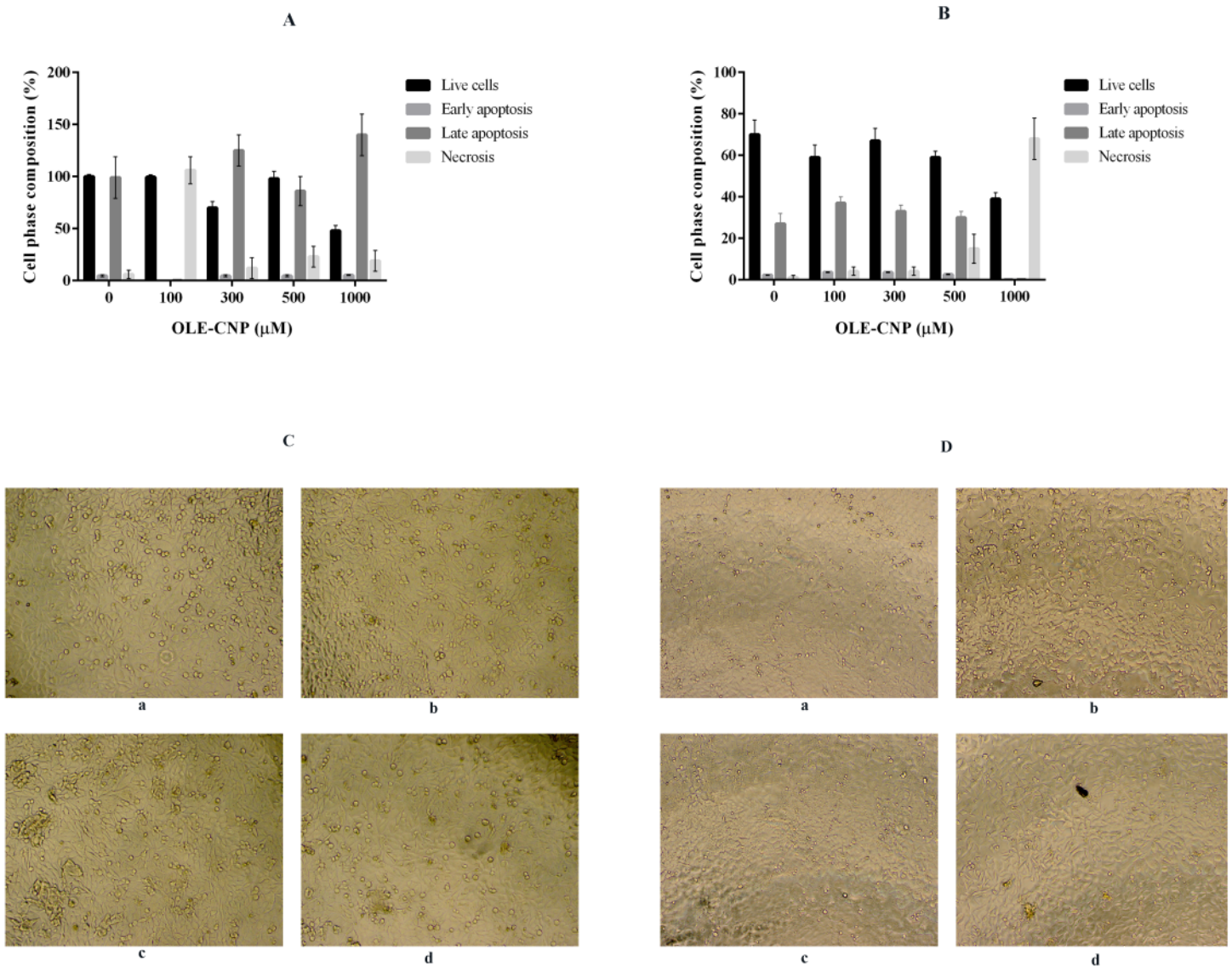

Figure 5

Apoptotic effect of OLE-CNPs on A549 (A) and MCF-7 (B), and optical microscopy images of A549 (C) and MCF-7 (D) cells treated with OLE (b), CNPs (c), OLE-CNPs (d) as well as untreated (control) cell lines (a).

Supplementary Files

This is a list of supplementary files associated with this preprint. Click to download.

- GraphicalAbstract.pdf